Wideband Black-Blood Cardiac Magnetic Resonance in Patients with Implantable Cardiac Devices

Pauline Gut, M.Sc.[1,2,3]; Hubert Cochet, Ph.D.[1,4]; Matthias Stuber, Ph.D.[1,2,5]; Aurélien Bustin, Ph.D.[1,2,4]

[1]IHU LIRYC, Heart Rhythm Disease Institute, Université de Bordeaux – INSERM U1045, Pessac, France
[2]Department of Diagnostic and Interventional Radiology, Lausanne University Hospital and University of Lausanne, Switzerland
[3]Faculty of Biology and Medicine, University of Lausanne, Switzerland
[4]Department of Cardiovascular Imaging, Hôpital Cardiologique du Haut-Lévêque, CHU de Bordeaux, Pessac, France
[5]CIBM Center for Biomedical Imaging, Lausanne, Switzerland

Introduction

The use of implantable cardiac devices (ICDs), such as implantable cardioverter defibrillators and pacemakers, is the most effective treatment for ventricular tachycardia, for heart failure, and for preventing sudden cardiac death [1, 2]. Use of these devices has been increasing over the past decades [3, 4], with approximately 1.4 million implantations occurring worldwide each year [5]. Cardiovascular magnetic resonance imaging (MRI) has become an essential diagnostic tool, due to its ability to generate high-resolution images of soft tissues without ionizing radiation. With the development of modern MR-compatible ICDs [6], the prevalence of patients with ICDs undergoing cardiovascular MRI has increased in recent decades. About 50%–70% of these patients will require follow-up MRI scans during their lifetime [7].

Bright-blood late gadolinium enhancement (LGE) imaging, such as phase-sensitive inversion recovery (PSIR) [8], is clinically routinely applied in patients for myocardial scar assessment, as it provides an excellent scar-myocardium contrast. However, the poor scar-blood contrast can challenge the detection and assessment of subendocardial, small, or focal scars. This scar-blood contrast can be improved using black-blood LGE imaging [9], which simultaneously darkens healthy myocardium and blood signals while enhancing scar signal using an appropriate inversion time (TI).

Thanks to technological advances, most implantable devices such as ICDs are now designed to be MR compatible[1], enabling wider clinical use of cardiac MRI in this patient population. However, the presence of ferromagnetic materials in the generator of these devices creates strong field inhomogeneities around the device. This results in bright-blood LGE images and black-blood LGE images that are heavily impacted by signal loss, hyperintensity artifacts, and image distortion, often resulting in non-diagnostic images [10]. In this article, we present the "wideband" MRI technique for reducing ICD-related artifacts, and its application to black-blood LGE imaging.

Theory

The inversion recovery pulse used in the PSIR and black-blood sequences and discussed in this article is an adiabatic hyperbolic secant radiofrequency (RF) pulse. An adiabatic hyperbolic secant pulse of duration T_p, amplitude modulation A(t), phase modulation ϕ(t), and frequency modulation ω(t) is described by the following equations:

$$B_1(t) = A(t)\, e^{-i\phi(t)}$$

$$A(t) = A_0\, sech(\beta t)$$

$$\phi(t) = \mu\, ln(sech(\beta t))$$

$$\omega(t) = \frac{d\phi(t)}{dt} = -\mu\beta\, tanh(\beta t)$$

with $-T_p/2 \le t \le T_p/2$ (seconds), A_0 the maximum B_1 field amplitude (micro tesla), β the frequency modulation parameter (radians per second), and μ the degree of phase modulation (dimensionless). The RF spectral bandwidth Δf of an adiabatic hyperbolic secant is determined by:

$$\Delta f = \frac{\mu\beta}{\pi}$$

[1]*The MRI restrictions (if any) of the metal implant must be considered prior to patient undergoing MRI exam. MR imaging of patients with metallic implants brings specific risks. However, certain implants are approved by the governing regulatory bodies to be MR conditionally safe. For such implants, the previously mentioned warning may not be applicable. Please contact the implant manufacturer for the specific conditional information. The conditions for MR safety are the responsibility of the implant manufacturer, not of Siemens Healthineers.*

Finally, to fulfil the adiabatic passage, the maximum B_1 field amplitude must satisfy the following condition:

$$A_0 \geq \frac{\mu\sqrt{\beta}}{\gamma}$$

with γ being the gyromagnetic ratio in Hz/Gauss. A smaller increase in μ and a larger increase in β can achieve a certain RF spectral bandwidth without a dramatic increase in the B_1 amplitude A_0.

ICD-related artifacts on LGE images

Implantable cardiac devices have ferromagnetic components with positive magnetic susceptibility. When placed in a magnetic field environment, the field lines are distorted around the cardiac device. This generates local field inhomogeneities, resulting in off-resonant spins (≠ Larmor frequency) with a frequency shift of 2 to 6 kHz of tissues located at 5 to 10 cm from the device generator [11]. When applying a bright-blood LGE sequence such as PSIR, the inversion recovery pulse used in the sequence will correctly invert spins at the Larmor frequency, but not off-resonant spins, as the frequency shift caused by the device may exceed the spectral bandwidth of the inversion pulse, typically around 0.8–1.1 kHz. This incorrect inversion results in a region of high signal intensity (bright region) caused by the mismapping of a disproportionate number of spins (MR signal) to this location during image reconstruction (Fig. 1). This abnormally bright region is known as a hyperintensity artifact, which often obscures the myocardium and compromises image quality and diagnosis. In addition, dephasing of protons on either side of the device generator boundary results in signal loss (dark region) (Fig. 1).

Banding artifacts can also be seen on PSIR LGE images in the presence of an ICD, and are associated with balanced steady-state free-precession (bSSFP) readout (Fig. 1A). The bSSFP readout relies on steady-state magnetization, which is achieved by rapidly repeating RF pulses with very short repetition times (TRs). The signal in bSSFP is a function of off-resonance frequency and varies periodically with off-resonance with a period of 1/TR. Field inhomogeneities (B0) cause phase accumulation between RF pulses. When the accumulation is a multiple of π, the signal nulls and dark bands appear [12]. A gradient recalled echo (GRE) readout can be used instead to avoid the banding artifacts when a cardiac implant is present (Fig. 1B). The GRE readout is much less sensitive to off-resonance since its signal does not periodically null with frequency offsets.

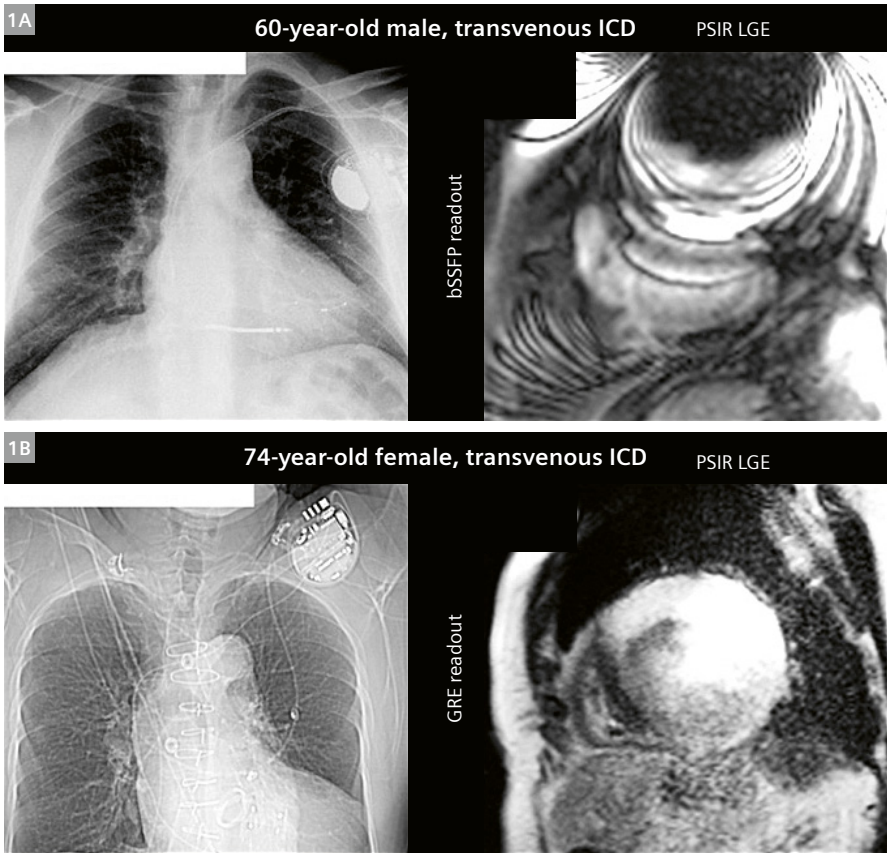

1 ICD-related artifacts on PSIR LGE images. **(1A)** Hyperintensity, signal loss, and bSSFP-associated banding artifacts. **(1B)** Hyperintensity and signal-loss artifacts, no banding artifacts with gradient echo readout.

Wideband bright-blood LGE

In 2014, Rashid et al. [11] introduced the concept of wideband PSIR LGE. They showed in their study a frequency shift of 2 to 6 kHz of tissues located at 5 to 10 cm from the device generator, which is well outside the standard spectral bandwidth of the 1.1 kHz inversion pulse. They therefore proposed to broaden the RF spectral bandwidth of the inversion pulse in the PSIR sequence from 1.1 to 3.8 kHz (μ = 16, β = 750 rad/s) (Figs. 2A, 2B). They showed that this RF spectral bandwidth broadening, known as wideband, enables the correct inversion of off-resonant spins, reducing or even eliminating hyperintensity artifacts that obscure the myocardium (Figs. 2C, 2D).

Wideband black-blood LGE

A black-blood LGE sequence can be achieved using inversion recovery followed by T2 preparation [13–15]. In this article, we present a 2D GRE black-blood sequence with inversion recovery (pulse duration = 10.24 ms) and T2 preparation (duration = 27 ms) (Fig. 3). The T2 preparation used is B1-insensitive and adiabatic, and consists of a 90°

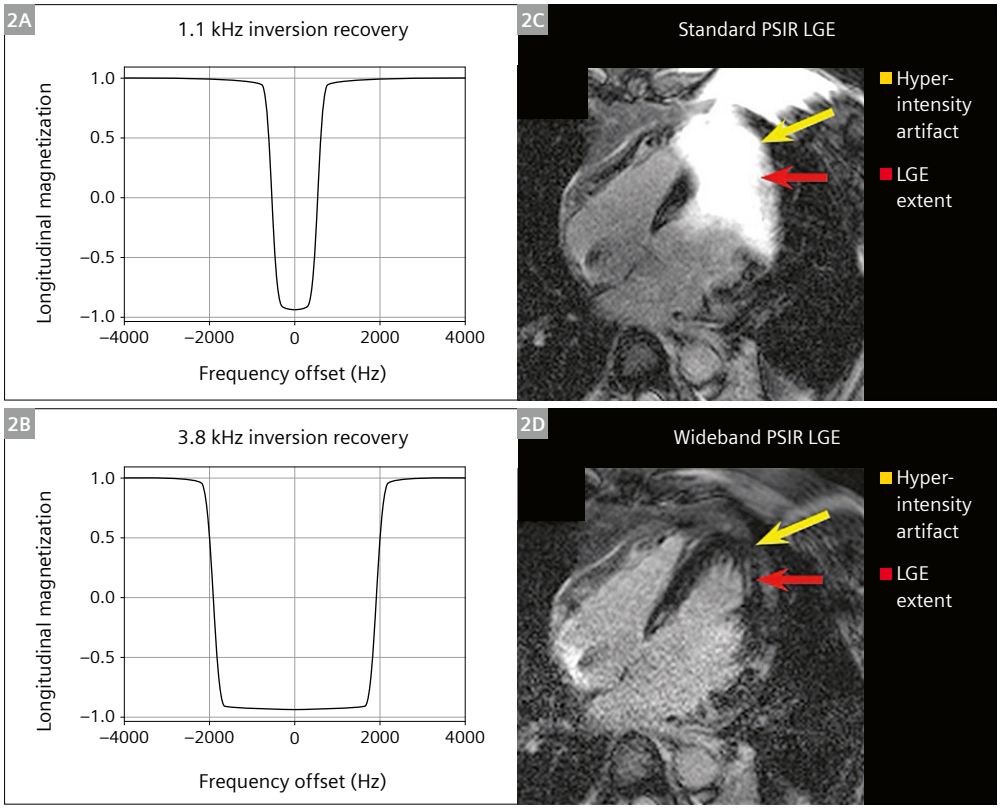

2 **(2A)** Standard spectral bandwidth of 1.1 kHz and **(2B)** wideband spectral bandwidth of 3.8 kHz of the inversion recovery pulse in the PSIR sequence, providing **(2C)** images with severe ICD-related hyperintensity artifacts and **(2D)** images with a net reduction in hyperintensity artifacts.

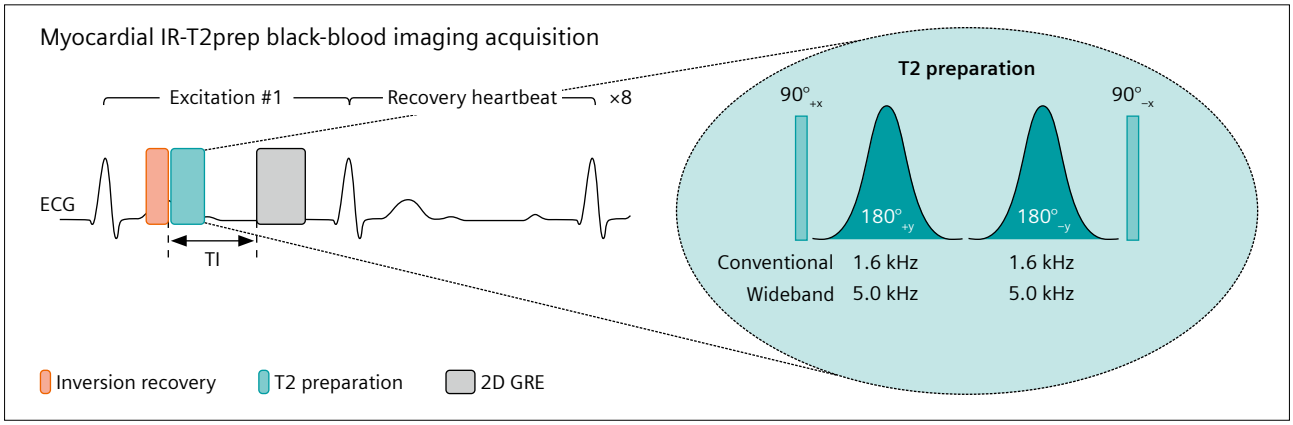

3 Myocardial IR-T2prep black-blood imaging framework, inversion recovery (IR) and T2 preparation pulses employed. Abbreviations: TI = inversion time; ECG = electrocardiogram; GRE = gradient echo.

tip-down RF pulse, two hyperbolic secant 180° refocusing RF pulses, and a 90° tip-up RF pulse [16] (Fig. 3). A spoiling gradient is then applied to suppress any residual transverse magnetization.

Similarly to PSIR, the spectral bandwidths used in the inversion recovery pulse (0.8 kHz), and the T2 preparation refocusing pulses (1.6 kHz) in the standard black-blood sequence are too narrow to properly prepare the magnetization in the presence of cardiac implants, resulting in LGE images with hyperintensities, signal loss, and image distortion (Figs. 4, 5). In 2024, wideband RF pulses were integrated into this black-blood LGE imaging to allow better LGE detection with reduced hyperintensity artifacts that obscure the myocardium in ICD patients [17] (Figs. 4, 5). It was proposed to broaden the spectral bandwidth of the inversion recovery from 0.8 to 3.8 kHz (μ = 16, β = 750 rad/s, A_0 = 19 μT), as proposed for wideband PSIR, and to broaden the spectral bandwidth of the T2 preparation refocusing pulses from 1.6 to 5.0 kHz (μ = 25, β = 785 rad/s, A_0 = 30 μT).

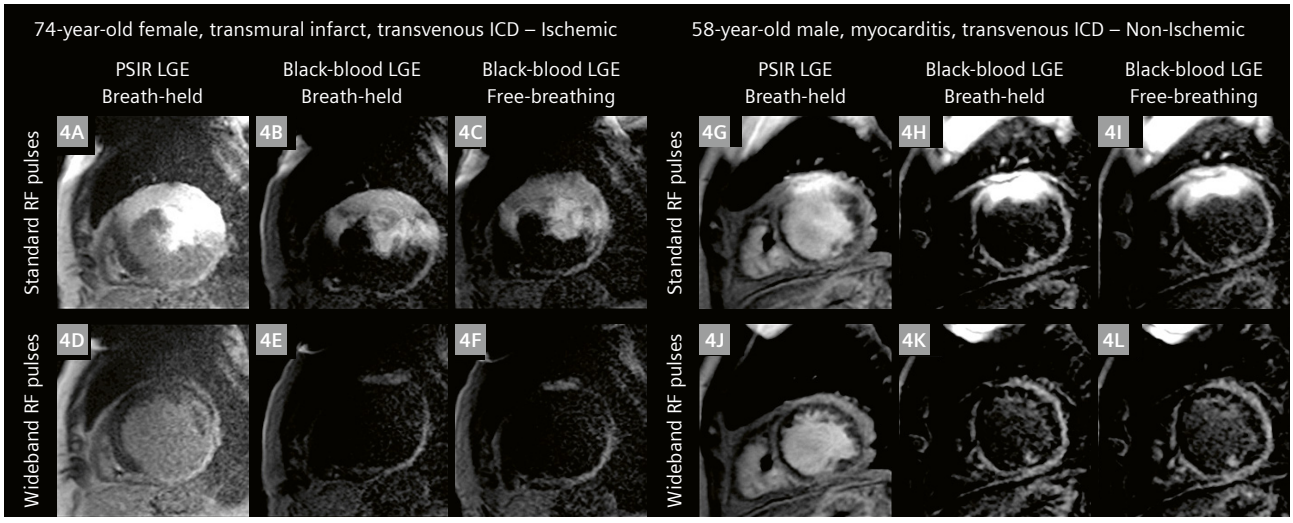

4 Cases 1 and 2. One female patient with ischemic infarct and one male patient with dilated cardiomyopathy with heart failure and reduced ejection fraction on probable myocarditis scar imaged at CHUV Lausanne University Hospital on a 1.5T MAGNETOM Sola system. Severe hyperintensities obscure the myocardium using standard PSIR LGE **(4A, 4G)** and standard black-blood LGE **(4BC, 4HI)**. These are suppressed using wideband PSIR LGE **(4D, 4J)** and wideband black-blood LGE **(4EF, 4KL)**.

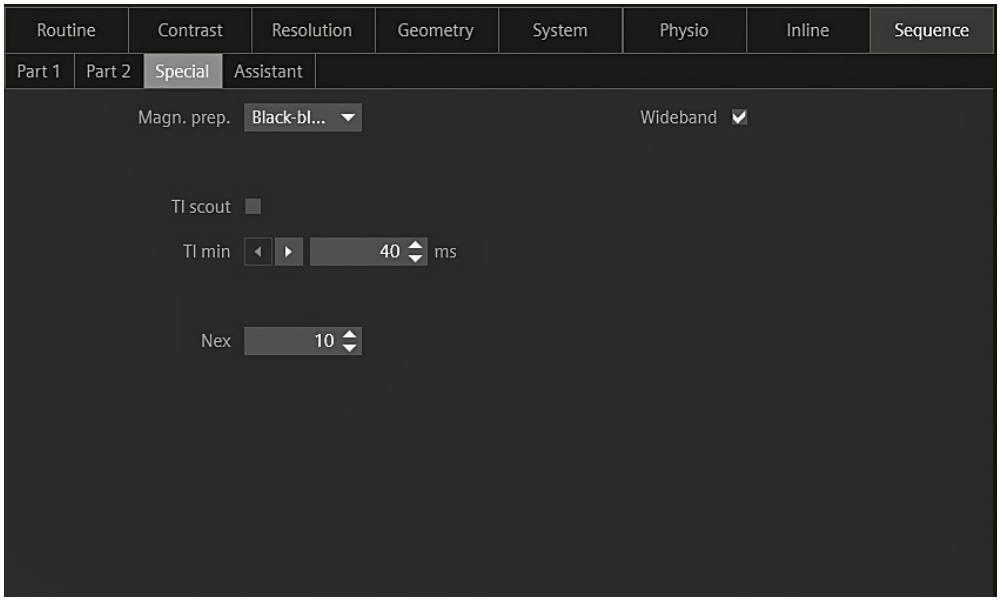

5 The Special card of the wideband black-blood sequence on a 1.5T MAGNETOM Sola system. Either PSIR or black-blood imaging can be chosen under "Magn. prep," not under "Contrast." Wideband RF pulses can be selected if the patient has an ICD. A TI scout can be performed for PSIR and black blood with or without wideband RF pulses. The number of excitations (Nex) is manually set and corresponds to the number of collected images for each slice position.

Tips and tricks for successful black-blood LGE imaging

Since its introduction, the 2D wideband black-blood GRE LGE sequence has been applied in a breath-hold study [17] and in a free-breathing study [18] with nonrigid motion correction at 1.5T (MAGNETOM Aera and MAGNETOM Sola, Siemens Healthineers, Erlangen, Germany). The protocol used is described in Table 1. It employs an electrocardiogram-triggered pulse to capture multiple single-shot images for each slice location during mid-diastole. In the special card of the protocol of the sequence at the MRI machine, PSIR or black-blood imaging can be chosen and wideband RF pulses can be activated or deactivated.

A dedicated TI scout can be performed with or without wideband RF pulses for both PSIR and black-blood LGE imaging. The optimal TI is then set to cancel to tissue of interest: black healthy myocardium for PSIR, and both black myocardium and black blood for black-blood imaging. The number of excitations (Nex) per slice location is determined manually (Fig. 5). A single short-axis slice is acquired within a single breath-hold or in free breathing with advanced non-rigid motion correction (Fig. 6), producing Nex images per slice position. The Nex images are then averaged, after motion correction if acquired in free breathing, into one high-quality image. A one-heartbeat gap between acquisitions allows for magnetization recovery. Below are some protocol recommendations:

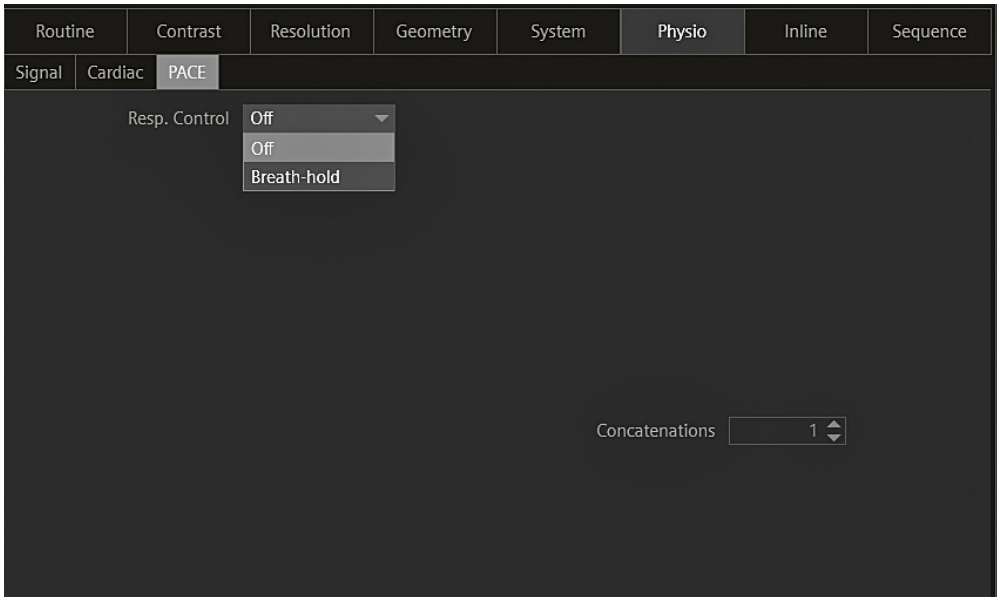

6 The Physio-PACE card of the black-blood imaging sequence on a 1.5T MAGNETOM Sola system. Images can be collected either during breath-hold or free breathing ("Resp. Control: Off"). In the case of free breathing, images will be delivered with motion correction (embedded in the reconstruction of the sequence).

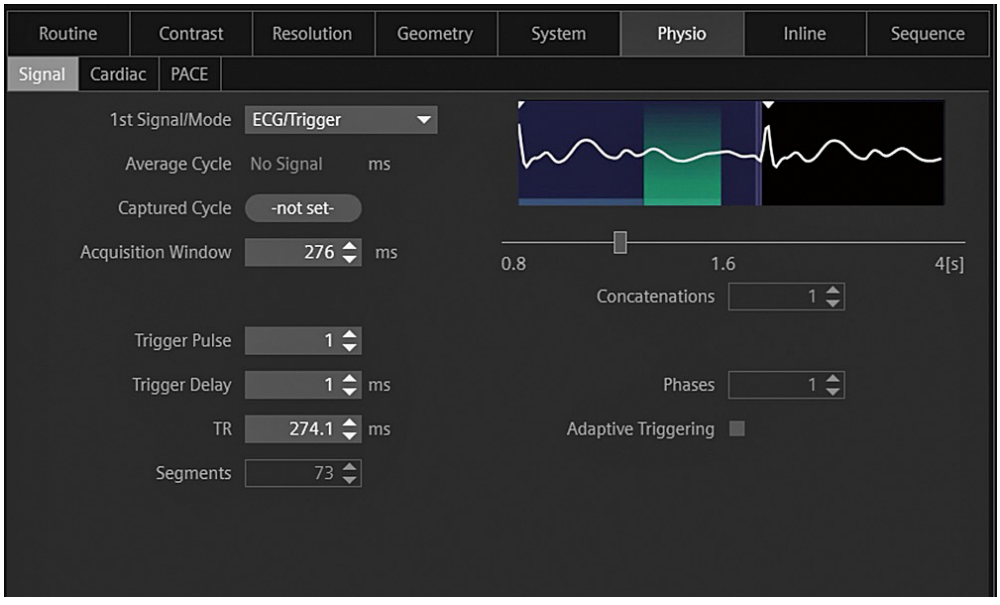

7 The Physio-Signal card of the black-blood imaging sequence on a 1.5T MAGNETOM Sola system. Images are collected during mid-diastole, and repetition time (TR) is set to the minimum.

1) We recommend collecting the images in mid-diastole (Fig. 7).
2) To achieve simultaneous darkening of healthy myocardium and blood signals, the correct TI needs to be determined with a dedicated wideband black-blood TI scout sequence (Fig. 5).
3) Regularly review the image contrast during acquisition (single-shot images are reconstructed and sent back to the operator on a beat-to-beat basis) and adjust the TI if necessary. Monitor the heart rate and adjust the trigger delay if necessary. Check for ghosting artifacts if performed in breath-hold, and check for wrapping artifacts.
4) Check for residual ICD-related hyperintensity artifacts obscuring the myocardium. If they are not completely suppressed, we recommend acquiring images with breath-hold during full inspiration to increase the heart-ICD distance. If this is not sufficient, the distance can be further increased by raising the patient's left arm and placing it next to their head.

MRI safety considerations

Before the 2000s, MRI was contraindicated in patients with any kind of cardiac implants (pacemaker, ICD, etc.). With the development of modern, smaller cardiac implants [6] with fewer magnetic components and improved electromagnetic interference safety, cardiac MRI has been shown to be safe at 1.5T with both MR-conditional and nonconditional cardiac implants [19–21] when following specific protocols and intraprocedural programming of the device [22–24]. The presence of fractured, abandoned, or epicardial leads still remains a contraindication to MRI.

Another aspect that has to be considered is the specific absorption rate (SAR). Wideband black-blood imaging is more SAR intensive than standard black-blood imaging, due to the increased B_1 amplitude in the inversion recovery and T2 preparation refocusing pulses. Wideband black-blood imaging is also more SAR intensive than wideband PSIR, due to the four additional RF pulses of the T2 preparation. For this prototype wideband black-blood imaging sequence at 1.5T, the proposed parameters (see Table 1) remained below the acceptable limit of 2 W/kg for clinical application, although SAR values were around 24 times higher than those of wideband PSIR. Nevertheless, a reassessment of the SAR deposit will be necessary for 3D applications.

Clinical applications

All images shown in this article were acquired by the Lausanne University Hospital on a 1.5T MAGNETOM Sola (software version *syngo* MR XA31 and XA51, Siemens Healthineers, Erlangen, Germany) and the University Hospital of Bordeaux on a 1.5T MAGNETOM Aera (software version *syngo* MR E11C) using a 32-channel spine coil and an 18-channel body coil.

Sequence setting	Parameter range
Acquisition	2D single-shot GRE
Cardiac control	ECG triggering
Respiratory control	Breath-holding
Spatial resolution	1.4 × 1.4 mm^2
Slice thickness	8 mm
Acquisition window	170–200 ms
Receiver bandwidth	751 Hz/pixel
Flip angle	15°
Paralell imaging	GRAPPA 2 with 36 reference lines
Phase FOV	75%
Phase resolution	76%
Partial Fourier	6/8
Asymmetric echo	Weak or Strong
Dummy heartbeats	0
k-space encoding	Linear
IR duration	10.24 ms
IR bandwidth	Conventional: 0.8 kHz; Wideband: 3.8 kHz
T2prep module	$90_x - 180_y - 180_{-y} - 90_{-x}$
T2prep duration	27 ms
T2prep refoc. bandwidth	Conventional: 1.6 kHz; Wideband: 5.0 kHz
Nex	5–10
Scan time	Nex * 2 heartbeats

Table 1: Wideband black-blood imaging sequence parameters. Abbreviations: ECG, electrocardiogram; FOV, field of view; GRAPPA, generalized autocalibrating partially parallel acquisitions; GRE, gradient recalled echo; Nex, number of excitations.

Findings in ischemic patients
In individuals with subendocardial or transmural infarct, wideband black-blood could improve LGE detection by 58% compared to wideband PSIR. This is explained by the contrast improvement at the scar-blood interface with the simultaneous darkening of healthy myocardium and blood. The improved scar detection was associated with an improvement in image quality of 5% [17, 18]. ICD-related hyperintensity artifacts were suppressed as well as with wideband PSIR, revealing LGE areas that may have been obscured.

Case 1: A 74-year-old female patient presenting with reduced left ventricular ejection fraction (20%), preserved right ventricular ejection fraction (48%), and a transvenous ICD. Severe hyperintensity artifacts hide half of the myocardium when using standard PSIR (Fig. 4A) and standard black-blood (Figs. 4B, 4C) LGE imaging, potentially masking the scar. Wideband sequences (Figs. 4D–4F) drastically reduced these artifacts, revealing all scarred segments with the presence of LGE in the inferior and inferolateral segments. The transmural LGE could be better manually segmented using wideband black-blood imaging than wideband PSIR. The application of nonrigid motion correction to black-blood LGE images obtained during free breathing resulted in sharp images (Fig. 4F).

Findings in non-ischemic patients
Dilated cardiomyopathy, hypertrophic cardiomyopathy, myocarditis, calmodulinopathy, and unknown-origin cardiomyopathy have been inspected with wideband black-blood LGE imaging, with midwall and subepicardial LGE findings. Overall, wideband black-blood LGE improved scar detection by 31%, with the same efficacy as wideband PSIR in suppressing ICD-associated hyperintensity artifacts. However, image quality was decreased by 8% compared to wideband PSIR, due to the lack of anatomical information [17, 18]. Scar localization with respect to the myocardial wall is challenged in black-blood imaging, due to the black healthy myocardium and blood signal. Therefore, especially for non-ischemic patients, bright-blood imaging remains essential to localize the LGE segments, whereas black-blood imaging is essential to detect the LGE segments. It is worth mentioning that these two acquisitions can be combined into a single sequence that provides coregistered bright- and black-blood LGE images.

Case 2: A 58-year-old male patient presenting with dilated cardiomyopathy with heart failure and reduced left and right ventricular ejection fraction (26% and 38%, respectively) on probable myocarditis scar. The patient was implanted with a transvenous ICD. Standard PSIR (Fig. 4G) and standard black-blood (Figs. 4H, 4I) LGE imaging revealed hyperintensity artifacts in the anteroseptal, anterior, and anterolateral segments. Wideband sequences (Figs. 4J–4L) were able to remove hyperintensity artifacts that masked the myocardium and LGE. Scar depiction was challenging with wideband PSIR, but improved markedly with wideband black-blood LGE imaging. The latter suggested strong evidence of subepicardial LGE in all segments. As in Case 1, the application of nonrigid motion correction to black-blood LGE images obtained during free breathing resulted in sharp images without ghosting artifacts (Figs. 4K, 4L).

What does the future look like?

Black-blood LGE imaging offers a significant advantage by improving LGE detection. However, as previously mentioned, accurate scar localization is essential for differentiating between ischemic and nonischemic cardiomyopathy, as well as for comprehensive pathological assessment. Bright-blood LGE plays a critical role in providing this spatial context but is acquired independently from black-blood LGE. A promising future direction involves combining these two techniques into a single integrated bright- and black-blood LGE sequence that enables coregistered imaging [25–27], as well as its 3D application.

Beyond distinguishing acute from chronic myocardial injuries with LGE, risk stratification in various myocardial diseases is vital for enhancing diagnostic and prognostic capabilities in structural heart disease. Cardiac parametric mapping, particularly T1 and T2 mapping, shows considerable promise in refining risk stratification in patients being evaluated for ICD therapy. These techniques may also enable longitudinal monitoring of myocardium post-ICD implantation, offering valuable insights into arrhythmic risk progression and supporting the tailoring of adjunctive therapies. The integration of parametric mapping with wideband RF pulses could be pivotal for quantitative cardiac MRI in ICD patients. Wideband T1 mapping has been proposed as a solution to the limitations of conventional T1 mapping in the presence of ICDs, though further clinical validation is needed [28, 29]. The feasibility of wideband T2 mapping in ICD patients has also been recently introduced but remains at an early stage of investigation [30]. Future preclinical and clinical studies are required to assess its sensitivity and specificity for detecting myocardial edema, acute inflammation, myocarditis, and takotsubo cardiomyopathy.

Conclusion

Magnetic resonance myocardial black-blood LGE imaging with wideband RF pulses holds significant promise for better LGE identification and characterization in ICD patients. The release of this C2P sequence could contribute to better LGE assessment in myocardial disorders in ICD patients and offer better access to cardiac MRI for this population.

Sequence availability

Our C2P sequence is currently available for sharing in *syngo* MR E11C, XA20, XA30, XA31, XA51, XA60, and XA61 on the C2P platform. The .exar1 protocol for the 1.5T MAGNETOM Sola (software version *syngo* MR XA61) is available to download on the MAGNETOM World website.

Acknowledgments

This research was supported by funding from the French National Research Agency under grant agreements Equipex MUSIC ANR-11-EQPX-0030, ANR-22-CPJ2-0009-01, and Programme d'Investissements d'Avenir ANR-10-IA-HU04-LIRYC, and by funding from the European Research Council (ERC) under the European Union's Horizon Europe research and innovation program (Grant Agreement No. 101076351).

References

1 Priori SG, Blomstrom-Lundqvist C, Mazzanti A, Blom N, Borggrefe M, Camm J, et al. 2015 ESC Guidelines for the management of patients with ventricular arrhythmias and the prevention of sudden cardiac death: The Task Force for the Management of Patients with Ventricular Arrhythmias and the Prevention of Sudden Cardiac Death of the European Society of Cardiology (ESC). Endorsed by: Association for European Paediatric and Congenital Cardiology (AEPC). Eur Heart J. 2015;36(41):2793–2867.

2 Ponikowski P, Voors AA, Anker SD, Bueno H, Cleland JGF, Coats AJS, et al. 2016 ESC Guidelines for the diagnosis and treatment of acute and chronic heart failure: The Task Force for the diagnosis and treatment of acute and chronic heart failure of the European Society of Cardiology (ESC)Developed with the special contribution of the Heart Failure Association (HFA) of the ESC. Eur Heart J. 2016;37(27):2129–2200.

3 Vaidya VR, Asirvatham R, Kowlgi GN, Dai MY, Cochuyt JJ, Hodge DO, et al. Trends in Cardiovascular Implantable Electronic Device Insertion Between 1988 and 2018 in Olmsted County. JACC Clin Electrophysiol. 2022;8(1):88–100.

4 Patel NJ, Edla S, Deshmukh A, Nalluri N, Patel N, Agnihotri K, et al. Gender, Racial, and Health Insurance Differences in the Trend of Implantable Cardioverter-Defibrillator (ICD) Utilization: A United States Experience Over the Last Decade. Clin Cardiol. 2016;39(2):63–71.

5 Kusumoto FM, Schoenfeld MH, Wilkoff BL, Berul CI, Birgersdotter-Green UM, Carrillo R, et al. 2017 HRS expert consensus statement on cardiovascular implantable electronic device lead management and extraction. Heart Rhythm. 2017;14(12):e503–e551.

6 Roguin A, Zviman MM, Meininger GR, Rodrigues ER, Dickfeld TM, Bluemke DA, et al. Modern pacemaker and implantable cardioverter/defibrillator systems can be magnetic resonance imaging safe: In vitro and in vivo assessment of safety and function at 1.5 T. Circulation. 2004;110(5):475–82.

7 Kalin R, Stanton MS. Current clinical issues for MRI scanning of pacemaker and defibrillator patients. Pacing Clin Electrophysiol. 2005;28(4):326–8.

8 Kellman P, Arai AE, McVeigh ER, Aletras AH. Phase-sensitive inversion recovery for detecting myocardial infarction using gadolinium-delayed hyperenhancement. Magn Reson Med. 2002;47(2):372–83.

9 Sridi S, Nuñez-Garcia M, Sermesant M, Maillot A, Hamrani DE, Magat J, et al. Improved myocardial scar visualization with fast free-breathing motion-compensated black-blood T1-rho-prepared late gadolinium enhancement MRI. Diagn Interv Imaging. 2022;103(12):607–617.

10 Gut P, Cochet H, Stuber M, Bustin A. Magnetic Resonance Myocardial Imaging in Patients With Implantable Cardiac Devices: Challenges, Techniques, and Clinical Applications. Echocardiography. 2024;41(11):e70012.

11 Rashid S, Rapacchi S, Vaseghi M, Tung R, Shivkumar K, Finn JP, et al. Improved late gadolinium enhancement MR imaging for patients with implanted cardiac devices. Radiology. 2014;270(1):269–74.

12 Bieri O, Scheffler K. SSFP signal with finite RF pulses. Magn Reson Med. 2009;62(5):1232–41.

13 Basha T, Roujol S, Kissinger KV, Goddu B, Manning WJ, Nezafat R. Black blood late gadolinium enhancement using combined T2 magnetization preparation and inversion recovery. J Cardiovasc Magn Reson. 2015;17(Suppl 1):O14.

14 Kellman P, Xue H, Olivieri LJ, Cross RR, Grant EK, Fontana M, et al. Dark blood late enhancement imaging. J Cardiovasc Magn Reson. 2016;18(1):77.

15 Basha TA, Tang MC, Tsao C, Tschabrunn CM, Anter E, Manning WJ, et al. Improved dark blood late gadolinium enhancement (DB-LGE) imaging using an optimized joint inversion preparation and T2 magnetization preparation. Magn Reson Med. 2018;79(1):351–360.

16 Nezafat R, Ouwerkerk R, Derbyshire AJ, Stuber M, McVeigh ER. Spectrally selective B1-insensitive T2 magnetization preparation sequence. Magn Reson Med. 2009;61(6):1326–35.

17 Gut P, Cochet H, Caluori G, El-Hamrani D, Constantin M, Vlachos K, et al. Wideband black-blood late gadolinium enhancement imaging for improved myocardial scar assessment in patients with cardiac implantable electronic devices. Magn Reson Med. 2024;92(5):1851–1866.

18 Gut P, Cochet H, Antiochos P, Caluori G, Durand B, Constantin M, et al. Improved myocardial scar visualization using free-breathing motion-corrected wideband black-blood late gadolinium enhancement imaging in patients with implantable cardiac devices. Diagn Interv Imaging. 2025;106(5):169–182. Epub 2024 Dec 12.

19 Nazarian S, Hansford R, Rahsepar AA, Weltin V, McVeigh D, Gucuk Ipek E, et al. Safety of Magnetic Resonance Imaging in Patients with Cardiac Devices. N Engl J Med. 2017;377(26):2555–2564.

20 Kim D, Collins JD, White JA, Hanneman K, Lee DC, Patel AR, et al. SCMR expert consensus statement for cardiovascular magnetic resonance of patients with a cardiac implantable electronic device. J Cardiovasc Magn Reson. 2024;26(1):100995.
21 Indik JH, Gimbel JR, Abe H, Alkmim-Teixeira R, Birgersdotter-Green U, Clarke GD, et al. 2017 HRS expert consensus statement on magnetic resonance imaging and radiation exposure in patients with cardiovascular implantable electronic devices. Heart Rhythm. 2017;14(7):e97–e153.
22 Nazarian S, Roguin A, Zviman MM, Lardo AC, Dickfeld TL, Calkins H, et al. Clinical utility and safety of a protocol for noncardiac and cardiac magnetic resonance Imaging of patients with permanent pacemakers and implantable-cardioverter defibrillators at 1.5 tesla. Circulation. 2006;114(12):1277–84.
23 Nazarian S, Halperin HR. How to perform magnetic resonance imaging on patients with implantable cardiac arrhythmia devices. Heart Rhythm. 2009;6(1):138–43.

Contact

Aurélien Bustin, Ph.D.
IHU LIRYC, Heart Rhythm Disease Institute
Avenue du Haut Lévêque
33000, Bordeaux
France
aurelien.bustin@ihu-liryc.fr

24 Nazarian S, Hansford R, Roguin A, Goldsher D, Zviman MM, Lardo AC, et al. A prospective evaluation of a protocol for magnetic resonance imaging of patients with implanted cardiac devices. Ann Intern Med. 2011;155(7):415–24.
25 Bustin A, Sridi S, Kamakura T, Jais P, Stuber M, Cochet H. Free-breathing joint bright- and black-blood cardiovascular magnetic resonance imaging for the improved visualization of ablation-related radiofrequency lesions in the left ventricle. EP Europace. 2022;24(Supplement_1).
26 de Villedon de Naide V, Maes JD, Villegas-Martinez M, Ribal I, Maillot A, Ozenne V, et al. Fully automated contrast selection of joint bright- and black-blood late gadolinium enhancement imaging for robust myocardial scar assessment. Magn Reson Imaging. 2024;109:256–263.
27 Richard T, de Villedon de Naide V, Nogues V, Génisson T, Narceau K, He K, et al. Improved and Automated Detection of Papillary Muscle Infarction Using Joint Bright- and Black-Blood Late Gadolinium Enhancement MRI. J Magn Reson Imaging. 2025. Online ahead of print.
28 Shao J, Rashid S, Renella P, Nguyen KL, Hu P. Myocardial T1 mapping for patients with implanted cardiac devices using wideband inversion recovery spoiled gradient echo readout. Magn Reson Med. 2017;77(4):1495–1504.
29 Hong K, Jeong EK, Wall TS, Drakos SG, Kim D. Wideband arrhythmia-Insensitive-rapid (AIR) pulse sequence for cardiac T1 mapping without image artifacts induced by an implantable-cardioverter-defibrillator. Magn Reson Med. 2015;74(2):336–45.
30 Gut P, Kim D, Cochet H, Sacher F, Jaïs P, Stuber M, et al. Wideband myocardial T2 mapping with implantable cardiac device: A preliminary evaluation in healthy volunteers at 1.5T. J Cardiovasc Magn Reson. 2025;27(Supplement 1):101276.